OPEN ACCESS
IOP Publishing
European Journal of Physics
Eur. J. Phys. **43** (2022) 035801 (8pp)
https://doi.org/10.1088/1361-6404/ac4d7c

Modeling in nuclear physics: a visual approach to the limitations of the semi-empirical mass formula

Miriam Hein*, Alexander Pusch and Stefan Heusler*

Institut für Didaktik der Physik, Westfälische Wilhelms-Universität Münster, Wilhelm-Klemm-Str. 10, 48 149 Münster, Germany

E-mail: miri.hein@gmx.de, alexander.pusch@wwu.de and stefan.heusler@wwu.de

Received 3 November 2021, revised 6 January 2022
Accepted for publication 20 January 2022
Published 16 February 2022

Abstract

The semi-empirical mass formula (SEMF) is a phenomenological model describing nuclear binding energies with high accuracy. We present different realizations and applications of this model based on 3D-printing and animations. A central new contribution is a visualization not only of the energy landscape provided by the SEMF, but also a comparison with actual experimental data. Our visualization of this *difference energy landscape* reveals limitations of the phenomenological model, and at the same time shows the special importance of the so-called magic numbers which have been explained in the shell model, introduced much later than the liquid drop model. This provides an excellent opportunity to discuss limits and merits of models in general in the context of physics education.

Keywords: 3D-printing, nuclear physics, modeling, binding energies, nuclide table, semi-empirical mass formula, video

(Some figures may appear in colour only in the online journal)

1. Introduction

Nuclear physics is a topic of central importance in modern physics, with a broad range of relevant applications, e.g. nuclear fusion and fission, or radioactive decay. As a generalization of the periodic table of elements, which classifies elements with respect to the number Z of

*Authors to whom any correspondence should be addressed.

0143-0807/22/035801+8$33.00 Printed in the UK

protons, isotopes are included with different number of neutrons N in the charts of nuclides such as the Karlsruhe Nuclid Chart, or the Chart of nuclides of the Brookhaven National Laboratory, which is also available online [1]. In order to understand the binding energy $E_B(Z,N)$ of a nucleus with a given number of protons Z, neutrons N, and total number of nucleons $A = Z + N$, the liquid drop model has been proposed by Gamov in 1930 [2]. Based on this model, the semi-empirical mass formula (SEMF) has been formulated in 1935 by Bethe and Weizäcker [3]. The model is based on several assumptions, in particular the nucleus is modeled as a round droplet of volume $V \propto A$ and radius $R \propto A^{(1/3)}$.

The explicit discussion of the role of models in physics, and in particular the ability to discuss the limits of models is an important topic in science education [4, 5]. Testing the accuracy of the liquid drop model and in turn of the SEMF in nuclear physics seems to be a good opportunity to explicitly discuss the role of models in modern physics. Moreover, modern computer animation helps to visualize the three-dimensional energy landscape of binding energies per nucleon $E_B(Z,N)/A$. Indeed, in recent time, many variants of visualizations of the binding energies have been proposed, e.g. using animations and even models within popular games such as Minecraft [6].

In the present contribution, we extend this work in two directions: on the one hand, 3D-printing technique is used in order to realize haptic models for binding energies per nucleon and radioactive decay, which can easily be reproduced in class.

In addition to the 3D-printed model, we produced a video showing the model assumptions of the SEMF, and its relation to magic numbers and the shell model by comparing the predictions of the SEMF with actual experimental data. We find new visualizations for the *difference energy landscape*, revealing limitations of the phenomenological model, in particular for small nuclei, and showing the special importance of the so-called magic numbers.

Within the nuclear shell model introduced by Goeppert-Mayer and by Jensen in 1949 [7], nuclei are particularly stable if the number of protons and neutrons coincides with the magic numbers. Note that magic numbers have been explained much later than the SEMF, thus it is striking to see that they can already be anticipated from the much simpler liquid drop model.

In combination, these models can be used in class for a detailed study not only of important topics in nuclear physics, but also in order to foster critical thinking concerning model building in modern physics in general.

2. From the semi-empirical mass formula to the magic numbers

The semi-empirical mass formula (SE) based on the liquid drop model of the nucleus describes the binding energy $E_B^{SE}(Z,N)$ as follows [4]

$$E_B^{SE} = a_V A - a_S A^{(2/3)} - a_C Z(Z-1)/A^{(1/3)} - a_A((Z-N)^2)/A - \delta(A,N)$$

with $\delta(A,N) = \pm a_P A^{-1/2}$ for nuclei with even (odd) number of protons *and* neutrons, otherwise $\delta(A,N) = 0$. The coefficients are determined empirically in order to optimally fit the experimental data. Using these coefficients, the binding energy per nucleon E_B/A can easily be visualized either as a 3D-printed energy landscape, or within a video, as shown in figure 1. The experimental data for the binding energy $E_B^{Exp}(Z,N)$ [5, 6] can be compared to the prediction of the model. For the realization as a 3D-printed model, we model the difference energy of the binding energy per nucleon given by $\Delta(Z,N) = E_B^{Exp}(Z,N)/A - E_B^{SE}(Z,N)/A$ as shown in figure 2. Using the model shown in figure 2, pupil can learn how to reflect the limit of validity of the liquid drop model: deviations between the liquid drop model and experimental

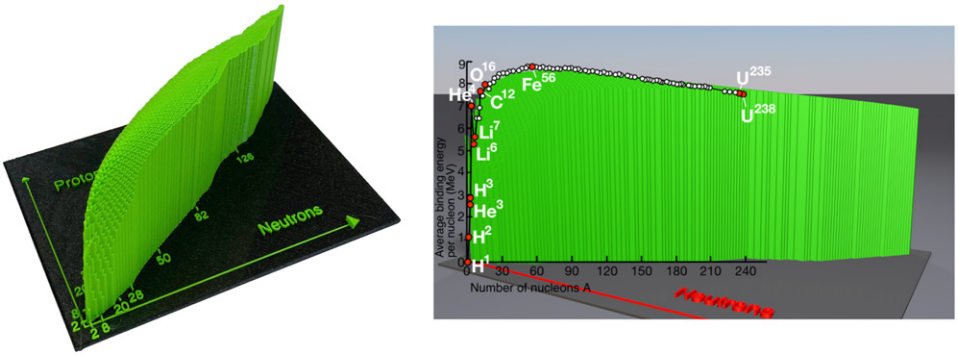

Figure 1. A 3D-printable model of the binding energies (left). The animation shows how the well-known 2D graph fits the 3D model (right).

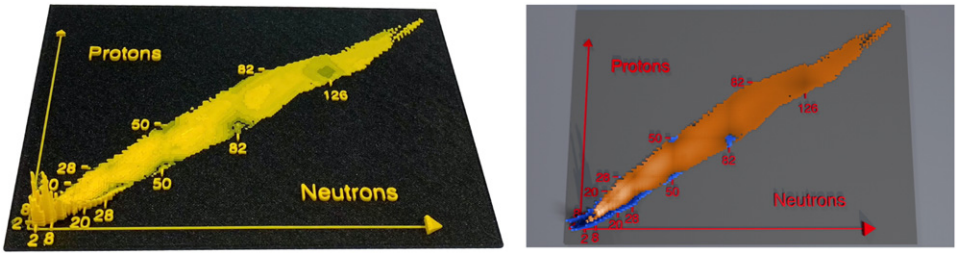

Figure 2. Difference of the binding energies per nucleon between the SEMF and experimental data, where magic lines and double magic numbers can be observed.

data are particularly large for small A. Here, the basic model assumption of a spherical droplet breaks down for small A. Indeed, the distinction between a volume term '$a_V A$ and a surface term' $a_S A^{(2/3)}$ breaks down in this case.

On the other hand, the deviations become particularly small for nuclei with magic numbers $2, 8, 20, 28, 50, 82, 126 \ldots$ [7] as can be observed both in the 3D-printed model and in the video, see also figure 6. If the number of protons and neutrons (Z, N) coincide with a magic number, the nucleus is called double-magic. Here, the difference energy $\Delta(Z, N)$ almost vanishes.

It is fascinating that the magic numbers, which have been explained within the nuclear shell model in analogy to the shell model of the bound electrons much later by Goeppert-Mayer and by Jensen in 1949 (Nobel price 1963), can already be anticipated from this *difference energy* landscape $\Delta(Z, N)$ comparing the experimental data and the SEMF of the binding energy per nucleon. The inner structure of shells is not included in the simple liquid drop model proposed in 1935. If the numbers of neutrons and protons coincides with the magic numbers, a certain number of shells is completely filled, and thus neglecting inner shell structures and the simple assumption of a spherical shape as proposed by the liquid drop model seem to be sufficient for the description of the binding energies in these cases.

3. Models for decay patterns in the charts of nuclides

The visualization of the binding energy as a three-dimensional energy landscape makes it possible to predict the stability of each nuclide. Since a nucleus, like all physical systems, tends to adopt the state of lowest energy, the condition for nuclear transformation is a release of energy to attain an energetically lower state. Due to the equivalence of mass and energy, this condition can be formulated as $\sum M_{\text{parent}} > \sum M_{\text{progeny}}$. In general, the mass $M(Z,N)$ of a nucleus is given by

$$M(Z,N) = Zm_Z + Nm_N - E_{\text{B}}(Z,N),$$

where m_Z, m_N are the masses of free neutrons and protons. Since $m_N > m_Z$, the free neutron itself is instable, and will decay into a proton, and electron and an antineutrino via β^--decay. In general, radioactive decay can only emerge through certain decay modes, the most important being α- and β-decay. So the main idea of the model is to provide all required information through the visualization of binding energy to identify radioactive and stable elements. However, care must be taken that a gain of binding energy is only a necessary condition, and not a sufficient condition for all decay modes. Note that e.g. for β^+-decay, the gain of binding energy must fulfil

$$E_{\text{B}}(Z-1,N+1) > E_{\text{B}}(Z,N) + (m_{e^+} + m_{\nu_e}) + (m_N - m_Z).$$

The allocation of small nuclei (until $A \approx 15$) is particularly suitable for a self-explaining model of radioactive decay, since the differences of the binding energies are most significant, such that the small effect of the mass of the electron and the neutrino is irrelevant in most cases. Each nuclide is represented as a tower, with its height proportional to its binding energy in an inverse representation, meaning that a lower tower implies a higher binding energy. On top of each tower is a removable grey box, which indicates the element, number of neutrons and protons as well as the mass number, as shown in figure 3.

The allowed movements to reach a lower tower (i.e. an element with a higher binding energy) are either α decay (emission of two protons and two neutrons), β^+ decay (a proton decays into a neutron, an anti-electron and a neutrino) or β^- decay (neutron decays into a proton, an electron and an anti-neutrino). The idea of the 3D model is to assign a certain decay mode or the stability of a nucleus based on the gain of binding energy. Therefore, the height of each element needs to be compared to potential progenies. In case a lower tower can be reached through a α, β^+ or β^- decay, the element can be marked with a ring according to the decay mode, which points to the progeny, as is visible in figure 4. Note that the fact that height difference is only a necessary but not a sufficient condition, which is a limitation of this model.

An element is stable if no lower tower can be reached using the motions allowed by the decay modes. The result is a self-assembled chart of nuclides, where the binding energy and allowed decay modes can be grasped haptically, see figure 5.

4. 3D-printing the models

A special feature of the model of the binding energies (section 2) is the color separation between the base plate and the nuclide map including the inscriptions on one level. This makes the models information stand out clearly (see figures 5 and 6).

Common FDM-3D-printers are able to produce multicolored prints in different ways:

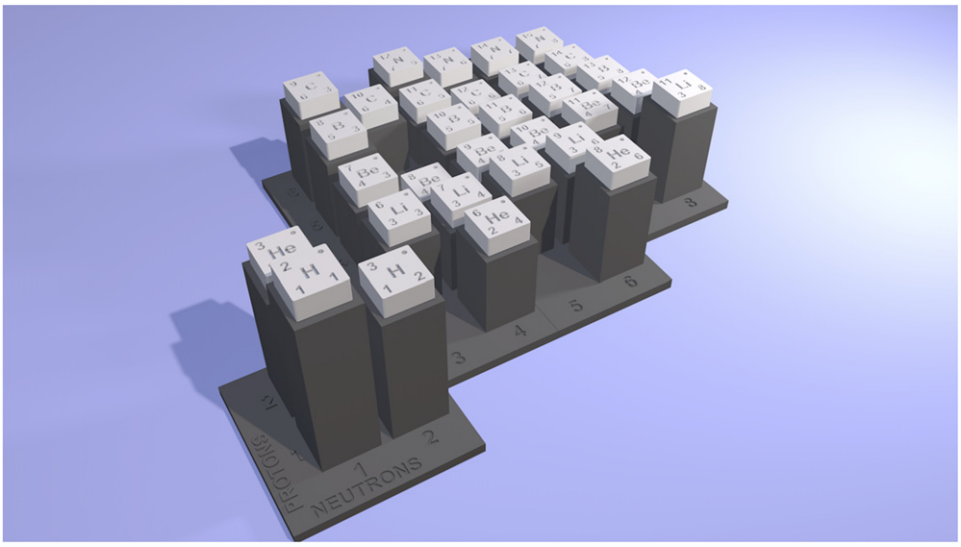

Figure 3. A 3D model of the binding energies per nucleon of the small nuclei to detect radioactive and stable elements.

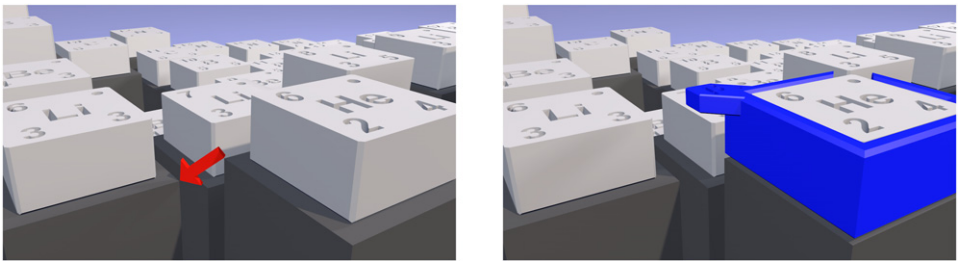

Figure 4. The decay mode of an element can be marked with a ring, which points to the progeny.

(a) Individual parts are printed separately in different colors and are connected by glueing or plugging (as in the decay models in section 3).
(b) For printers with multiple nozzles (or with interchangeable magazines), two (or more) different colored filaments can be used at alternately.
(c) The filament can be changed during printing at a specific height (z-level). Depending on the machine, a specific code can be added to g-code, that pauses the machine at a certain height. See e.g. https://prusaprinters.org/color-print/ for details.

With this model, the color change can be implemented particularly easily, since the change between the colors takes place from a certain cutting plane. To do this, the printer can be paused at a suitable point during the printout and the filament can be changed to another color (variant (c)). Many slicers offer the function of adding a pausing command to a certain height.

The printable files for the presented models can be obtained under https://physikkommunizieren.de/semf/.

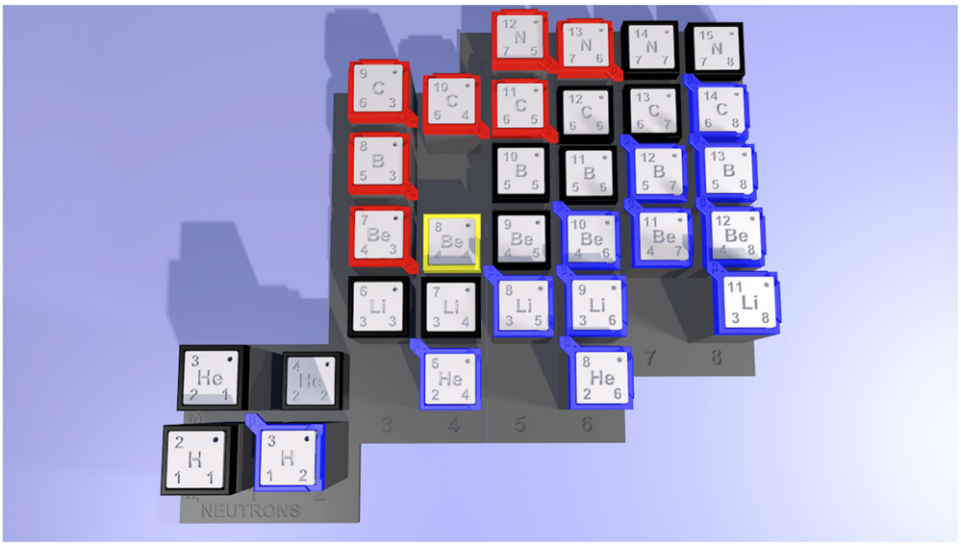

Figure 5. The composed 3D nuclides chart visualizes decay series and stable elements based on binding energy.

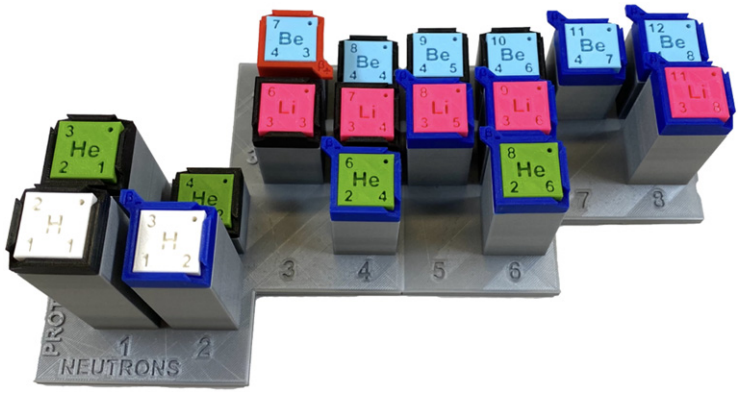

Figure 6. A 3D printed model of the binding energies of the small nuclei with placeable caps (e.g. H, He, Li) and decay markers (black: stable, blue: XXX, red: XXX).

5. Video

In order to show the magnitude of the five contributions to SEMF, we produced a video (https://physikkommunizieren.de/semf/) where the terms are visualized one by one in a dynamic animation. Furthermore, we compare to experimental data in the difference energy plot. In such a way, the deviations between theory and experiment can be visualized in an intuitive manner, which can serve as a starting point for a general discussion on models and model building in physics.

6. Conclusion and outlook

In this contribution, we discussed properties and limits of physical models using 3D-printing and animation techniques at the example of nuclear physics.

Printed models offer learners additional haptic access to the object, which fascinates learners and invites them to explore. The 3D-printed models proposed here have two possible applications: on the one hand, using the model shown in figure 1, pupil can understand many fundamental properties of nuclear reactions, e.g. why, depending on the number A of nucleons, either fusion reactions (like in our Sun) or fission reactions (like in nuclear power stations) lead to a gain of energy. Concerning radioactive decay, the model allows for predictions of decay series. Since the element iron is in the minimum of the energy landscape, it is the most stable elements of all.

Animations are particularly useful for dynamical visualizations. Here, for the first time, we shown an animation of the difference energy landscape comparing the predictions of the liquid drop model with actual experimental data. In such a way, the particular importance of magic numbers is revealed, since for these cases, the accuracy of the SEMF is particularly high, which can be read off directly from the animation.

While the rapid development in computer graphics allows for a large variety of illustrations of physical models, the nature of models itself is not self-obvious for pupils [8, 9]. Thus, further empirical research concerning model understanding and its relation to various possible representations is in need. We believe that models in nuclear physics provide a good example for abstract model building in physics, and thus might serve as a starting point for further research in this field.

Acknowledgments

We are grateful to Professor C Weinheimer for advisory in processing the experimental data of nuclear binding energies.

ORCID iDs

Miriam Hein https://orcid.org/0000-0002-2621-9698
Alexander Pusch https://orcid.org/0000-0001-5407-8469
Stefan Heusler https://orcid.org/0000-0002-5686-9560

References

[1] National Nuclear Data Center (NNDC) Chart of nuclides (Brookhaven) https://nndc.bnl.gov/nudat3/
[2] Gamow G 1930 Mass defect curve and nuclear constitutions *Proc. R. Soc.* A **126** 632–44
[3] Weizäcker C F 1935 Zur Theorie der Kernmasse *Z. Phys.* **96** 431–58
[4] Clement J 2000 Model based learning as a key research area for science education *Int. J. Sci. Educ.* **22** 1041–53
[5] Ubben M and Heusler S 2019 Gestalt and functionality as independent dimensions of mental models in science *Res. Sci. Educ.* **49** 1–15
[6] Binding Blocks, Department of Physics https://york.ac.uk/physics/public-and-schools/secondary/binding-blocks/
[7] Velusamy R 2007 Mayer–Jensen shell model and magic numbers *Resonance* **12** 12–24

[8] Pluta W J, Chinn C A and Duncan R G 2011 Learners' epistemic criteria for good scientific models *J. Res. Sci. Teach.* **48** 486–511
[9] Ubben M and Heusler S 2018 A haptic model of vibration modes in spherical geometry and its application in atomic physics, nuclear physics and beyond *Eur. J. Phys.* **39** 045404